



# Large-eddy simulation of formation of three-dimensional aeolian sand ripples in a turbulent field

WU ChuiJie<sup>1†</sup>, WANG Ming<sup>2</sup> & WANG Liang<sup>3</sup>

With the method of large-eddy simulation, the equation of spherule motion and the method of immersed boundary condition, numerical simulations of three-dimensional turbulent aeolian motion and the formation of sand ripples under three-dimensional turbulent wind and the mutual actions of saltation and creeping motion were carried out. The resulting sand ripples have the form that is flat on the upwind side and steep on the leeward, which is identical to the sand ripples in nature. We also realized the self-restoration process of three-dimensional sand ripples, which shows the correctness of the method of numerical simulation and the models of saltation and creeping. Finally, We analyzed the influence of sand ripples on the three-dimensional turbulent wind field, and found that due to the appearance and development of sand ripples, in the normal direction of ground there exists stronger energy exchange, and moreover, there is close correspondence between the forms of sand ripples and the vorticity close to the ground surface.

large-eddy simulation, equation of spherule motion, sand ripples, saltation, creep

#### 1 Introduction

As a significant global environment problem, desertification has received extensive attention. The desertification leads to land degradation in agricultural productivity, and loss of large areas of fertile land resources. It may also threaten industries, transportation, basic infrastructures and human lives and cause substantial economic damage. The desertification directly causes the generation of sand storms, which not only leads to serious casualties and property loss, but also greatly affects the quality of communication and power transmission.

Received November 16, 2007; accepted April 6, 2008

doi: 10.1007/s11433-008-0118-2

<sup>†</sup>Corresponding author (email: <u>cjwudut@dlut.edu.cn</u>)

Supported by the Key Project of National Natural Science Foundation of China (Grant No. 10532040)

State Key Laboratory of Structural Analysis for Industrial Equipment, Dalian University of Technology, Dalian 116024, China;

<sup>&</sup>lt;sup>2</sup> Yellow River Institute of Hydraulic Research, Zhengzhou 450003, China;

<sup>&</sup>lt;sup>3</sup> Research Center for Fluid Dynamics, Science School, PLA University of Science and Technology, Nanjing 211101, China

The main presentation form of desertification is the aeolian motion of sand, which is the origin of soil erosion and sand storms. Therefore, the research of the mechanism of aeolian motion has attracted great attention. It is shown that there is no other way to understand the mechanism of wind erosion, transportation and deposition of sand particles and the process of desertification than to fully understand the mechanical mechanism of aeolian motion.

Aeolian sand ripples are the basic landforms under the effect of wind, which are closely related to the transportation process of sand and are the basis of understanding other aeolian landforms. Traditionarily, based on the conclusions of field observations and wind tunnel experiments, some experiential formulae are used to describe the variation of sand bed and fluid field, and by a simple solution process the formation and the evolution processes of sand ripples were revealed [1-3]. With the development of computer science, the method of numerical simulation gradually becomes an important method in the study of formation mechanism of aeolian sand ripples.

The numerical simulation of aeolian sand ripples started in the mid 1980s. Anderson<sup>[4–6]</sup> first applied the theoretical model of collision to numerically simulate the formation of sand ripples. Their results preliminarily recovered the formation process of sand ripples in nature, but there are a few disadvantages, e.g. the simulation is two-dimensional, which did not consider the motion of sand in the span-wise and the discreteness of attack angles, and assumed all saltation sands rebound; this is not seen in nature. In the simulation, it is assumed that the velocity of wind and saltation particles is in a steady state, without considering unsteadiness of velocity and direction of wind and the feedback effect of sand on the wind field.

Recently, Zheng's research group carried out a fruitful study of aeolian sand motion. Zheng et al. [7] obtained the collision model of sands with ground, the initial jumping velocity, the distribution of probability density of horizontal velocity and rotational angular velocity of sands.

Zheng et al. [8] gave the distribution of concentration of sand along the height in aeolian flow, and indicated that the concentration is not simply an exponential decay with the height. Zheng et al. [9] carried out the wind tunnel test of electrified sand particles in an aeolian flow and found the rule and distribution of aeolian electric field for the first time, demonstrated the relations of charge-mass ratio and strength of electric field with the wind speed and particle sizes, and at the same time showed the influence of electrified sand particles on the saltation of sands.

Nishimori and Ouchi<sup>[10]</sup>, using a very simple method and considering the effect of saltation and creeping on the formation of sand ripples, successfully reproduced the formation and evolution process of aeolian sand ripples on a small scale.

Walter and Werner<sup>[11]</sup> put out a 3-D computational model for aeolian sand ripples. They pointed out that the results obtained with Anderson's and Kennedy's models are contradictory with the results of in-field observation and numerical simulations, because among small sand ripples there is nonlinear merging taking place.

Nino and Atala<sup>[12]</sup> proposed a simplified 2-D discrete model. In their model the forces on a single particle on the sand bed were studied in detail, and the moving speed of sand ripples was found to decrease with the increase of wave height.

Wang et al. [13,14] simulated 2-D sand ripples with three models of saltation, creeping and stable state. Sun and Wang [15] gave another explanation of the formation of sand ripples. They found that in the motion the sand particles constantly collide with each other, and since the exchange of momentum happens in a very short time, the impulsive force is much larger than the gravity, drag and friction forces between sands, and only the change of velocity needs to be taken into account at

this very short moment. Based on this consideration, they built a discrete model of particle dynamics, which includes sand-sand and sand-fluid actions.

As mentioned above, it can be found that much work has been done on the process of aeolian saltation and the formation of sand ripples, but none studied these two motions together as a whole system. Since in nature, the saltation of sand particles and the formation of landform are two sides of a system, and they interact with each other, any research that separates these two parts will be incomplete. The goal of this study is to combine them together, in order to understand the generation and evolution of 3-D sand ripples under the mutual actions of turbulent aeolian saltation and creeping motion and the self restoration process of 3-D sand ripples.

## 2 Numerical algorithm of large-eddy simulation of turbulence and the verification of code

The pseudo-spectrum method is used to numerically solve the incompressible Navier-Stokes equations and continuous equation to get the background wind field. When the wind carrying sands moves in the air, the reaction of sands to the wind field is realized by means of the immerse boundary method.

#### 2.1 Numerical algorithm

The filtered non-dimensional continuous equation and momentum equations of incompressible flow with constant density are as follows, respectively:

$$\begin{cases}
\frac{\partial \overline{u}_{j}}{\partial x_{j}} = 0, \\
\frac{\partial \overline{u}_{i}}{\partial t} + \frac{\partial}{\partial x_{j}} \overline{u}_{i} \overline{u}_{j} = -\frac{\partial \overline{p}}{\partial x_{i}} + \frac{1}{Re_{\tau}} \frac{\partial^{2} \overline{u}_{i}}{\partial x_{j} \partial x_{j}} - \frac{\partial \tau_{ij}}{\partial x_{j}} + F_{i}(t),
\end{cases} \tag{1}$$

where  $\tau_{ij} = R_{ij} - \frac{1}{3}\delta_{ij}R_{kk}$ ,  $R_{ij} = \overline{u_iu_j} - \overline{u_i}\overline{u_j}$ ,  $Re_{\tau}$  is the Reynolds number based on the friction velocity on the wall,  $\frac{1}{3}\delta_{ij}R_{kk}$  are isotropic turbulent stresses, and  $F_i(t)$  are the reaction force of immerse boundaries to the flow, as can be found in eq. (6).

To make the equations close, one should adopt proper models for the sub-grid stress  $\tau_{ij}$ . In this study, we use the Smagorinsky vortex viscosity model as follows:

$$\tau_{ij} = -2\nu_{\tau} \left( \overline{S}_{ij} - \left\langle \overline{S}_{ij} \right\rangle \right), \tag{2}$$

where

$$\begin{bmatrix}
\overline{S}_{ij} = \frac{1}{2} \left( \frac{\partial \overline{u}_i}{\partial x_j} + \frac{\partial \overline{u}_j}{\partial x_i} \right), \\
v_{\tau} = (c_s \Delta)^2 |\overline{S}|, \\
\Delta = (\Delta_1 \Delta_2 \Delta_3)^{1/3}, \\
|\overline{S}| = \left[ 2 \left( \overline{S}_{ij} - \langle \overline{S}_{ij} \rangle \right) \left( \overline{S}_{ij} - \langle \overline{S}_{ij} \rangle \right) \right]^{1/2}.
\end{bmatrix} (3)$$

 $\langle \ \rangle$  is the plan averaged on the plane parallel to the ground.

For the space discretization of control equations (1), in span-wise and stream-wise directions, the spectrum method is applied, and along the vertical direction the central difference algorithm with second order precision is used. For the time marching, the Crank-Nicolson semi-implicity algorithm is used for the viscous terms, and for the convection terms, the Adams-Bashforth algorithm is applied. The details of numerical method can be referred to ref. [16].

The computational area is  $2\pi \text{ m} \times \frac{4}{3}\pi \text{ m} \times 1 \text{ m}$ , and the orthogonal meshes are used. The grid numbers are  $64 \times 64 \times 64 \times 64$ . In stream-wise and span-wise directions, uniform grids are applied, and in the direction perpendicular to the ground, the uneven grids which are denser to the ground are used, and the rule of distribution of grids is shown in eq. (4). Let  $x_3$  be the non-dimensional coordinate vertical to the ground,  $-1 < x_3 < 0$ , and in this direction, the grid number is  $N_3$ , then the positions of local grids can be found with the help of the following formula:

$$x_{3,j} = \frac{1}{\alpha} \operatorname{th} \left( \xi_j \operatorname{th}^{-1} \alpha \right), \tag{4}$$

where  $\xi_j = -1 + (j-1)/(N_3-1), j=1, 2, \cdots, N_3$ , and  $\alpha$  is an adjustable parameter,  $0 < \alpha < 1$ .

The larger the value of  $\alpha$ , the denser the grids to the ground. Within the viscous sublayer ( $z^+ < 11$ ), there are at least four grids, where  $z^+ = z_w u_\tau / v$  is the coordinate of the wall, and  $z_w$  is the distance to the ground.

For the boundary conditions, in the stream-wise and span-wise directions, there are periodical boundaries, respectively; on the ground, the non-slip boundary condition is applied, and the top boundary is a free slip boundary. In span-wise and stream-wise directions, there must be enough sand ripples contained in the computational region, and the results show that this requirement is met. Since the motion of sands mainly is close to the ground surface, we choose a vertical height of the computational region that contains most of suspended sands.

Since the initial condition of real wind field is unknown, firstly, we take the velocity distribution of a traditional boundary layer as the initial condition, then after a while when the averaging wind field almost reaches the steady state, we write down the velocity distribution of wind field and use it as the initial field in the computation carried out afterward. Within this initial wind field, it contains regular and irregular disturbances.

#### 2.2 The moving boundary method

When the sand moves in the wind field driven by the wind, it produces a reaction force to the flow, and affects the wind field. Therefore, the wind field and sands together constitute a two-way coupling system. And moreover, due to the motion of sands, the shape of landform changes constantly, which forms a moving boundary problem. It is clear that using the method of body-fitting moving meshes to study the sand motion and the changes of shape of landform is unrealistic, since the scale of sands is too small and the amount of sands is too large. In this study, the reaction of sands to the wind field and the changes of landform shape are treated with the method of immerse moving boundary.

The method of immerse moving boundary is a kind of Eulerian-Lagrangian method. The control equations of flow are solved in the fixed Cartesian coordinates, and the moving boundaries are tracked in the Lagrangian way. There are two advantages of using the immerse boundary method, i.e., on the one hand, it greatly simplifies the grid generation process; on the other hand, it does not need special treatment of control equations, and is very easy to be used in the program.

The immerse boundary method is first put forth by Peskin<sup>[17]</sup>, in order to simulate the heart beat and blood flow. Whereafter, researchers made a lot of efforts to improve this method. The key point of this method is how to put the boundary conditions to the immerse boundary, which is also the sign that one immerse boundary method distinguishes from the other ones. According to the different ways of treating boundary conditions, the methods of immerse boundary can be divided into two classes<sup>[18]</sup>, which are the methods of continual force field and discrete force field, respectively. In this study, we use the method of continual force field.

Among existing methods, when dealing with the elastic boundary and the rigid boundary, the treatment method is different, but the basic idea is the same, i.e., construct a reaction force and add it to the momentum equations, to reflect the boundary effect on the flow.

For the rigid boundary, the method put forward by Goldstein et al. [19] is a typical one. The reaction force representing the effect of rigid fixed boundary is defined as

$$F(t) = \alpha \int_0^t \mathbf{u}(\tau) d\tau + \beta \mathbf{u}(t), \tag{5}$$

where u(t) is the velocity of flow field at the immerse boundary. From the physical point of view, it can be explained as a damping vibrator.

For the rigid moving boundary, the reaction force can be defined as

$$F(t) = \alpha \int_0^t [\mathbf{u}(\tau) - \mathbf{u}_b(\tau)] d\tau + \beta [\mathbf{u}(t) - \mathbf{u}_b(t)], \tag{6}$$

where F(t) is the reaction force of the resultant force of sands to the flow, as shown in the next section, and  $u_b(t)$  is the velocity of flow field at the immerse boundary. The fixed rigid boundary can be viewed as a special case with  $u_b(t) = 0$ .

According to Newton's first law of motion, the force of a sand particle acting on the wind is equal to that of wind acting on the sand particle. Since the size of the sand particle is much smaller than the size of a grid, we only decompose the reaction force to the vertexes of the grid where the sand particle is located; in other words, the influence of every sand particle is limited within one grid.

### 3 Physical models

#### 3.1 Saltation model

First, let's analyze the forces acting on a single particle of sand, in order to get the control equations of sand motion.

Set up the coordinate oxyz as shown in Figure 1. Suppose a spherical sand particle with diameter D and density  $\rho_g$  moves in the space, and its equation of motion is the Newton's second law of motion. The forces acting on a sand particle in the air with the motion of saltation are the drag of air, the Saffman force, the Magnus force, the Basset force, the virtual mass force and the gravity force, but among them the most important forces are the gravity  $F_g$  and drag  $F_d$ . Besides, the influences of lift  $F_l$ , the Magnus force  $F_m$ , and the electrostatic force  $F_e$ , etc. on the motion of sand are also not neglectable.

For a spherical sand particle, the gravity of sand  $F_{\rm g}$  can be shown as

$$F_{\rm g} = -mg = -\frac{1}{6}\pi D^3 \rho_{\rm g} g,\tag{7}$$

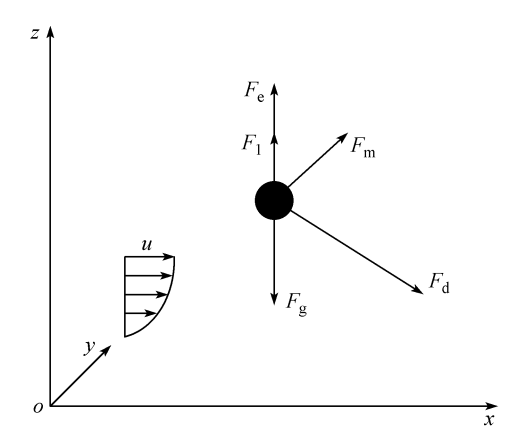


Figure 1 The forces acting on a sand particle.

where  $\rho_g = 2650 \text{ kg/m}^3$ .

Whether the sand in ascend or descend motion, the drag  $F_{\rm d}$  is the function of velocity  $V_{\rm r}$ , and its direction is the same as the one of relative velocity, which can be shown as

$$F_{\rm d} = 0.5C_{\rm d}A\rho_{\rm a}V_{\rm r}V_{\rm r},\tag{8}$$

where  $V_{\rm r} = [(\dot{x}_{\rm p} - u)^2 + (\dot{y}_{\rm p} - v)^2 + (\dot{z}_{\rm p} - w)^2]^{1/2}$ ,  $\boldsymbol{u}$  is the wind speed at the location of the sand,  $\dot{\boldsymbol{x}}_{\rm p}$  is the position of the sand,  $A = \frac{\pi}{4}D^2$  is the area of the cross section of the sand, the density of air is  $\rho_{\rm a} = 1.23$  kg/m<sup>3</sup>, and  $C_{\rm d}$  is the coefficient of drag, which is a function of  $Re_{\rm r}$ . Here we use the empirical formula of White<sup>[20]</sup>:

$$C_{\rm d} = \frac{24.0}{Re_{\rm r}} + \frac{6.0}{1.0 + \sqrt{Re_{\rm r}}} + 0.4,$$
 (9)

where  $Re_r = \frac{V_r D}{v}$ , and v is the kinematic viscosity of air,  $v = 1.46 \times 10^{-5}$  m<sup>2</sup>/s.

The Magnus force is generated by the rotate motion of sand and the viscosity of fluid, which is shown as [21]

$$\boldsymbol{F}_{\mathrm{m}} = \pi \rho_{\mathrm{a}} \frac{D^{3}}{8} (\boldsymbol{\omega} \times \boldsymbol{V}_{\mathrm{r}}). \tag{10}$$

In this study, the rotating speed  $\omega$  of sand is set between 0 to 600 rad/s.

When studying the orbit of motion of a sand particle in saltation, Anderson and Hallet believed that the lift is generated by the shear stress, and the pressure gradient results in the shear stress that is orthogonalized in the direction of velocity increasing, hence the value of the resulting lift  $F_1$  can be expressed as

$$F_{\rm l} = \frac{1}{2} \rho_{\rm a} C_{\rm l} A [(u_{\rm top}^2 - u_{\rm bot}^2) + (v_{\rm top}^2 - v_{\rm bot}^2) + (w_{\rm top}^2 - w_{\rm bot}^2)], \tag{11}$$

where  $u_{\text{top}}$ ,  $v_{\text{top}}$ ,  $w_{\text{top}}$  and  $u_{\text{bot}}$ ,  $v_{\text{bot}}$ ,  $w_{\text{bot}}$  are the velocities of air at the top and the bottom of sand, respectively,  $C_1$  is the coefficient of lift, and usually it can be set to  $0.85C_d$ .

Based on experimental results, Schmidt et al. [23] put forward the formula of aeolian electric field

E, i.e.,

$$E(z) = 51000.0(100.0z)^{-0.6}. (12)$$

The electrostatic force produced by this electric field on the sand is

$$F_{ez} = mcE(z_{\rm p}),\tag{13}$$

where c is the charge-mass ratio, i.e., the charge carried by every kilogram of sands. In this study, we take it between  $-60 \mu C/kg$  and  $60 \mu C/kg$ .

After the detailed analysis of the forces acting on a sand particle, we can obtain the equation of motion of a saltation sand particle as

$$\begin{cases}
m \frac{d^{2} x_{p}}{dt^{2}} = f_{1} = -F_{dx} + F_{mx}, \\
m \frac{d^{2} y_{p}}{dt^{2}} = f_{2} = -F_{dy}, \\
m \frac{d^{2} z_{p}}{dt^{2}} = f_{3} = -mg - F_{dz} + F_{mz} + F_{ez} + F_{l}.
\end{cases}$$
(14)

The initial condition is

$$t = 0: x_{p} = 0, \ y_{p} = 0, \ z_{p} = -1, \ \dot{x}_{p} = 0, \ \dot{y}_{p} = 0, \ \dot{z}_{p} = w_{p0}.$$
 (15)

When simulating the saltation motion of sand particles, the Lagrange method is used to trace the track of every particle in saltation motion. The fourth order Runge-Kutta method is used to numerically solve the motion equations of saltation of sand particles, coupled with the control equations of wind field, to get the tracks of saltation of sand particles. The procedure of numerical simulation is as follows:

- (1) Setup the initial positions of sand particles  $x_{p0}$ ;
- (2) Solve the control equations of wind field to obtain the solution of flow field;
- (3) Decide in which mesh unit the particle  $x_{p0}$  is located, and get the coordinates of eight vertexes of the cuboid unit that contains the particle  $x_{p0}$ , then from the solved flow field, one can get the velocities of these eight points;
  - (4) From these eight velocities, the fluid velocity  $u_a$  of  $x_{p0}$  can be obtained with interpolation;
- (5) Put the velocity of fluid  $u_a$  into the control equations of saltation of sand to get the saltation velocity of sand particles  $u_p$ ;
- (6) Use the time step  $\Delta t$  and the saltation velocity of sand particles  $u_p$  to get positions of sand particles  $x_{p1}$ :

$$\mathbf{x}_{\mathrm{pl}} = \mathbf{x}_{\mathrm{p0}} + \mathbf{u}_{\mathrm{p}} \Delta t. \tag{16}$$

Let

$$\boldsymbol{x}_{\text{p0}} = \boldsymbol{x}_{\text{p1}}.\tag{17}$$

951

- (7) Output  $x_{pl}$ ;
- (8) From eq. (14), one can get the force acting on a sand particle, then interpolate the force onto the eight vertexes of the mesh unit where the particle is located;

#### (9) Repeat (2)—(8) to get the tracks of all saltation sand particles.

In the computation, sometime sands could move out of the computational region. Therefore, it is necessary to setup the boundary condition of saltation particles, together with the boundary condition of flow field. Since in the stream-wise and spanwise directions, the flow field has periodical boundary conditions, therefore in these two directions, the boundary conditions of saltation particles are also set to be periodical; at the bottom the boundary condition is a non-slip one; for the top boundary, since there are very few particles flying out of the boundary, they will be directly discarded once they exit.

Let the computational region of sand bed be  $2\pi \text{ m} \times \frac{4}{3}\pi \text{ m}$ , and the number of sand particles

usually reaches the order of  $10^9$ . It is not difficult to trace each particle, but it needs a huge amount of computation to trace all particles in the simulation. Even with parallel computation, the time needed is still unbearable. In order to solve this problem, we put forward a model of sand mass, which is in concept similar to that of fluid particle, i.e., a sand mass contains a lot of sand particles but from the macroscopic point of view, it is still small enough to be treated as a mass point. We set the maximum number  $n_{\text{max}}$  of particles contained in a sand mass, then use a random number r to stochastically decide the number of sand particles  $n_r$  contained in the sand mass, i.e.,  $n_r = n_{\text{max}} r$ ,  $r \in (0,1]$ .

When the wind blows over a flat ground, every sand particle on the surface has the possibility to jump up, but on the ground with concavo-convex shape, the sand particles on the upwind side jump up, and those on the leeward deposit. Therefore, we first randomly choose the positions of sand particles that jump up, and then determine whether it is on the upwind side. If it is not, then repeat the above process, i.e.,

$$\begin{cases} x_{p0} = l_x r, \\ y_{p0} = l_y r, \\ z_{p0} = z(x_{p0}, y_{p0}), \end{cases}$$
 (18)

where  $x_{p0}$ ,  $y_{p0}$ ,  $z_{p0}$  is the initial coordinate of jumping sand, respectively;  $l_x$ ,  $l_y$  is the length of the computational region in x, y direction, respectively; r is a random number;  $z_{p0}$  is the coordinate of particle  $(x_{p0}, y_{p0})$  in z direction, which means that once sand particles jump up and move in a saltation style, the thickness of sand bed will be different, i.e., the surface shape of sand bed will become curved.

Because the mechanism of sand jumping up is still unknown, in our physical models we do not consider the details of the jumping process. But the jumping speed can be obtained with the help of the distribution function of sand's jumping speed. Li-Hong He at Lanzhou University examined a lot of distribution functions of vertical jumping speed of sand, and found that the Weibull distribution function is the best one, therefore in our study we use Weibull distribution function as the distribution function of vertical speed  $w_{p0}$ , as shown below:

$$F(w_{p0}, \alpha, \beta) = 1 - e^{-\left(\frac{w_{p0}}{\beta}\right)^{\alpha}}, \tag{19}$$

where  $\alpha$  and  $\beta$  are the shape parameter and the scale parameter of Weibull distribution function,

respectively.  $\alpha$  and  $\beta$  for different diameters of particles and wind speeds can be found in ref. [24]. After the distribution function of vertical jumping speed was determined, the initial jumping

speed of each particle can be found. Let  $F(w_{p0}, \alpha, \beta) = r$ , where r is a random number, and putting it into eq. (19), one can get the vertical jumping speed of sand particles as

$$w_{\rm p0} = \beta \Big[ \ln(1 - r_{\rm random})^{-1} \Big]^{\frac{1}{\alpha}}.$$
 (20)

The horizontal jumping speeds  $u_{p0}$  and  $v_{p0}$  are always zero. From eq. (20), we can find the initial jumping speed of every sand particle. In order to examine whether or not the jumping speed is consistent with Weibull distribution, we show the statistical result of vertical jumping speeds of 100000 particles in Figure 2, compared with the Weibull distribution function. From the figure, it is clear that the statistical result of eq. (20) is in good agreement with Weibull distribution.

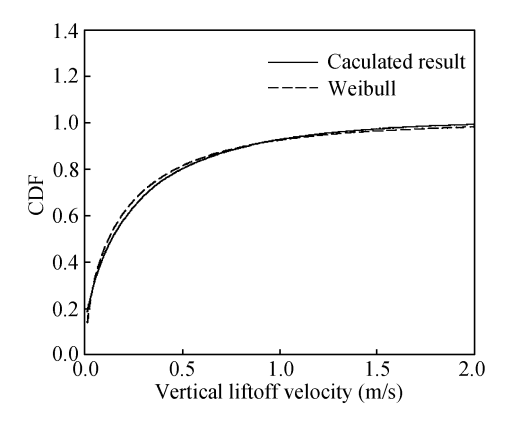


Figure 2 The comparison of our statistical result with Weibull distribution.

Finally, let's determine the number of jumping particles in every time step as
$$n = sA\Delta t, \tag{21}$$

where n is the number of particles which jump up in the period of time of  $\Delta t$ , s is the rate of jumping particles, and A is the area of the sand bed.

#### 3.2 Creeping model

(i) Creeping velocity. For the creep motion, we use the Eulerian method, i.e., view the creeping velocity of sand particles in the sand bed as a velocity field, which is obtained via the velocity of wind above the sand bed, under the reaction of sand ripples to the wind field.

The forces driving the creeping sand particles are the pressure force of wind ahead and the impact force of saltation particles. We assume that the creeping motion is driven by the pressure force of wind ahead alone, then the creeping velocity is the function of wind velocity as

$$\begin{cases} u_{c} = f_{u}(u, v, w), \\ v_{c} = f_{v}(u, v, w), \\ w_{c} = 0, \end{cases}$$
 (22)

where u, v, w are the velocities at the locations of creeping particles, and the vertical creeping velocity is set to zero. Due to the complexness of creeping motion, the mechanism involved is still unknown, and thus it is impossible to get the precise expressions of  $f_u(u, v, w)$  and  $f_v(u, v, w)$ . In

this study, we follow the way of try-and-correct, i.e., firstly assume an expression of creeping velocity, then correct it with the comparison of results with the nature phenomenon. If they agree well, then it means that the expression is basically correct; otherwise, make correction and do it again.

In this study we let  $f_u(u, v, w) = u_{i-1}$  and  $f_v(u, v, w) = v_{i-1}$ , then the equation of creeping velocity takes the form:

$$\begin{cases} u_{c} = u_{i-1}, \\ v_{c} = v_{i-1}, \\ w_{c} = 0, \end{cases}$$
 (23)

where  $u_{i-1}$  and  $v_{i-1}$  are the velocities at the upwind nodes of the mesh where the creeping particle is located, respectively.

In the computation, the sand bed is divided into two-dimensional grids on the x-y plane, which are consistent with the grids of wind field on x-y section. At the initial time, the number of particles in each grid is the same, i.e., at first the sand bed is flat, and sand particles lay one by one and layer by layer. Using the previously got creeping velocity field and assuming that all particles on the surface join the creeping motion, the creeping velocities of particles in the same grid are the same; then using the creeping velocity and the time step, we can get the positions of particles on the surface. In this way, one can find which particle moves into which grid, and then at next time step, the new creeping velocity of that grid is used to find the new creeping velocity.

(ii) The boundary condition on the ground surface. Under the mutual action of saltation and creeping motions, the ground surface is no longer flat, and becomes wavy and rugged. If we still set the boundary condition at certain height to be non-slip, then the effect of landform on the flow field cannot be taken into account. Therefore, the immerse boundary method is used to reflect the reaction of changing landform to the flow field. For the grids under the ground surface, their velocities are set to be zero.

#### 4 Analysis of results

#### 4.1 The evolution process of three-dimensional sand ripples

Figure 3 shows the complete evolution process of sand ripples. In Figure 3(a), there are no sand ripples appearing, but only very small wavy rugae on the sand bed. In Figure 3(b), there appear small sand ripples, but their heights are rather low. From Figures 3(c) to (f), the sand ripples gradually develop, the outlines become clear and the heights of sand ripples rise. From Figures 3(g) and (h), it can be seen that the height and the length of sand ripples have essentially no change, which indicates that the sand ripples have reached a fully developed stage and gradually settled down.

The two sections of sand ripples in Figure 4 are taken from Figures 3(g) and (h) at y = 0.59, respectively. From the figure, it is clear that the height and the length of sand ripples do not change, and the sand ripples move ahead as a whole, which indicates again that the sand ripples have reached a fully developed stage. The average height of sand ripples is 8 mm, and the shapes of upwind side of sand ripples are flat, and the ones on the lee side are steep, which are identical to the ones found in nature.

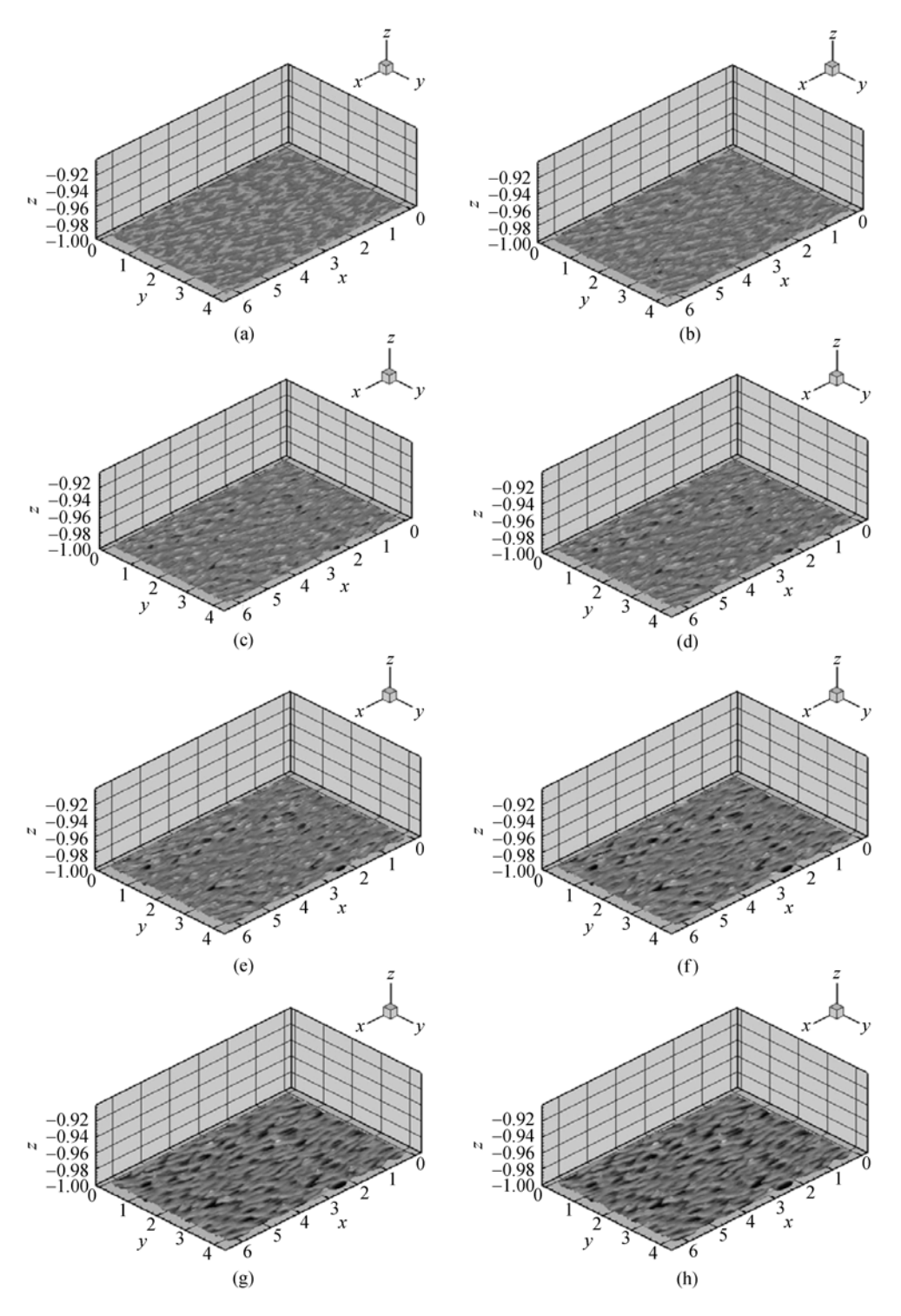


**Figure 3** The evolution process of sand ripples. (a) t = 0.109 s; (b) t = 0.391 s; (c) t = 0.800 s; (d) t = 1.081 s; (e) t = 1.217 s; (f) t = 1.327 s; (g) t = 1.392 s; (h) t = 1.440 s.

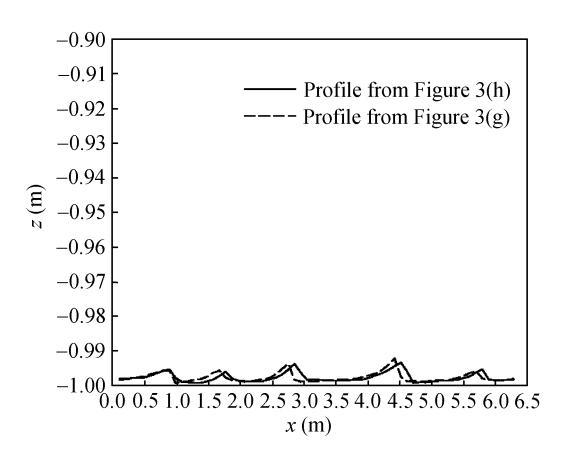


Figure 4 The sections of sand ripples.

#### 4.2 The self-restoration process of sand ripples

In nature, the sand ripples are the typical physical substances that have the property of nonlinear self-organization. For example, wiping off a square area of sand ripples on the surface of desert and waiting for a while, the wiped sand ripples will reappear, which are very naturally mergered with surrounding sand ripples and show no sign of having been wiped out.

Here, we reproduce this process numerically. In Figure 5, after sand ripples appear, we wipe out a square area of sand ripples, then let the simulation go on. After a while, at the place where sand ripples have been wiped out, the sand ripples gradually reappear, and finally completely merge into surrounding sand ripples. This numerical experiment shows from the other point that the numerical method and the saltation and creeping models used in this study are correct and reasonable, by which one can recover the typical physical feature of evolution of sand ripples.

#### 4.3 The influence of sand ripples on the flow field

Next, let's take a look at the interactions of near ground turbulent field and sand ripples. In fact, on the one hand, sand ripples are the imprints of near ground turbulent field on the surface of desert; on the other hand, sand ripples can also influence the structures of near ground turbulent field.

Figure 6 is the vector diagram of a section of turbulent field, at y = 1.69 m and t = 2.2 s. From the figure, one can find that since at different positions along x axis the heights of sand ripples are different, the different wind profiles are produced.

Since in a boundary flow, all characteristic lengths are functions of positions along the stream-wise direction, it is impossible to give a unique Reynolds number. But from Figure 6, we can use the approximated average thickness of the boundary layer (about 0.045 m), average wind speed (10 m/s) and the kinematic viscosity of air ( $\nu = 1.46 \times 10^{-5}$  m<sup>2</sup>/s) to estimate the Reynolds number at the moment, which is about 30822.

Figure 7 shows the streamlines in the wind section of y = 1.96 in the area of 0-10 cm above ground surface at different moments, and on the background it is the distribution of spanwise vorticity. We can find from the figures that at beginning the streamlines are rather calm, and there is almost no vertical velocity in the field; along with the increase of heights of sand ripples, the vertical velocity gradually increases, and when the heights of sand ripples reach 8 mm, the air flow in the vertical direction is very violent, so the variation of landforms is an important factor which influences the saltation motion of sands.

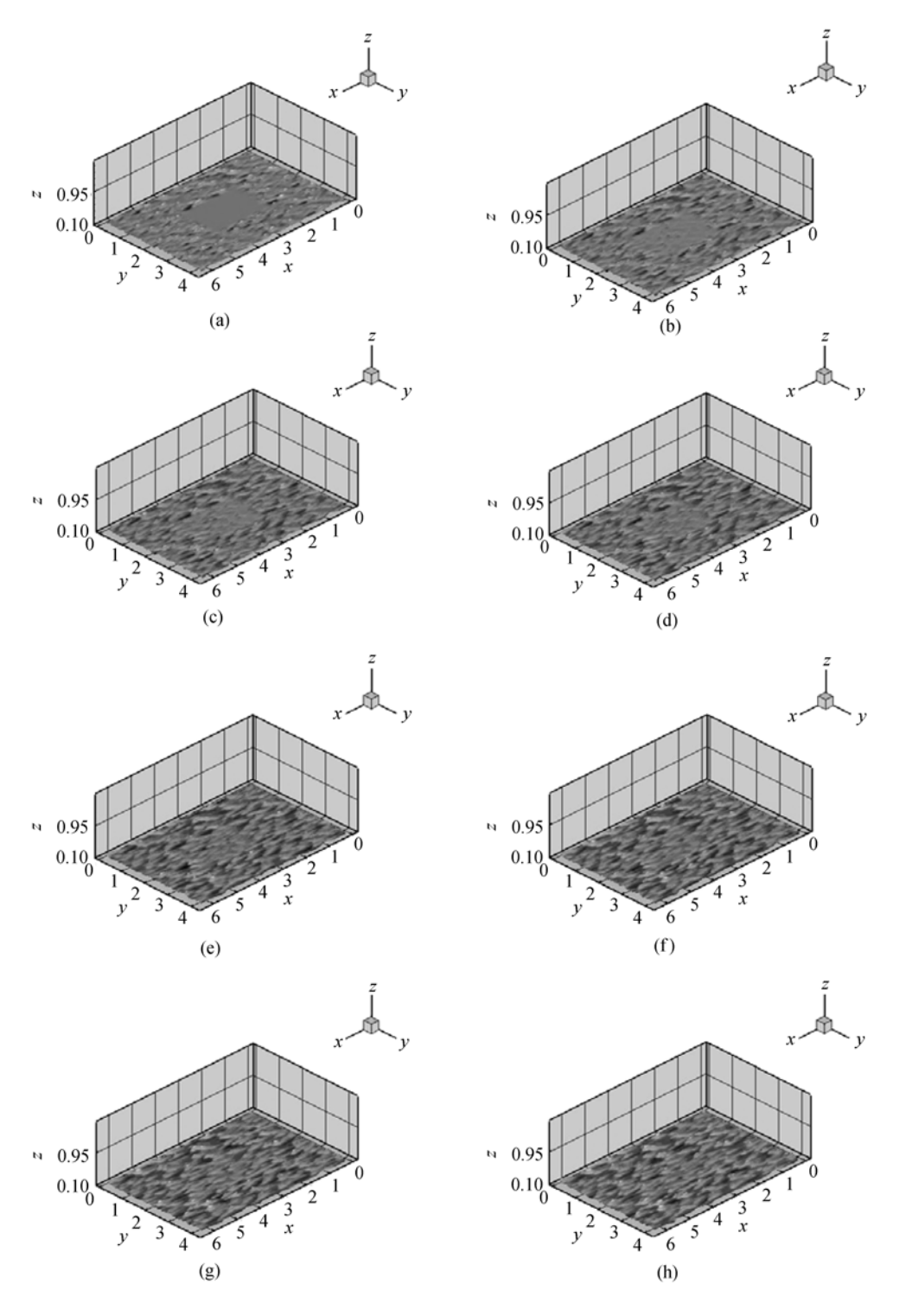


**Figure 5** The self-restoration process of sand ripples. (a) t = 0.556 s; (b) t = 0.804 s; (c) t = 1.110 s; (d) t = 1.261 s; (e) t = 1.361 s; (f) t = 1.475 s; (g) t = 1.594 s; (h) t = 1.751 s.

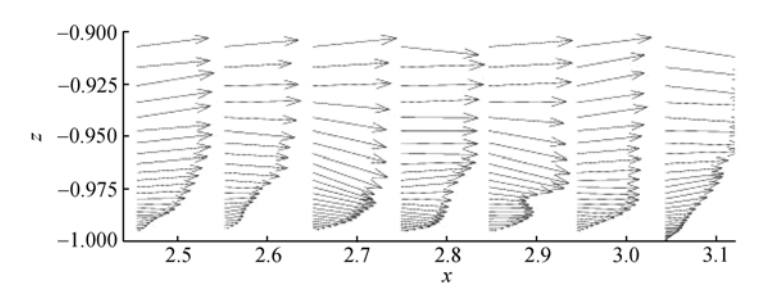
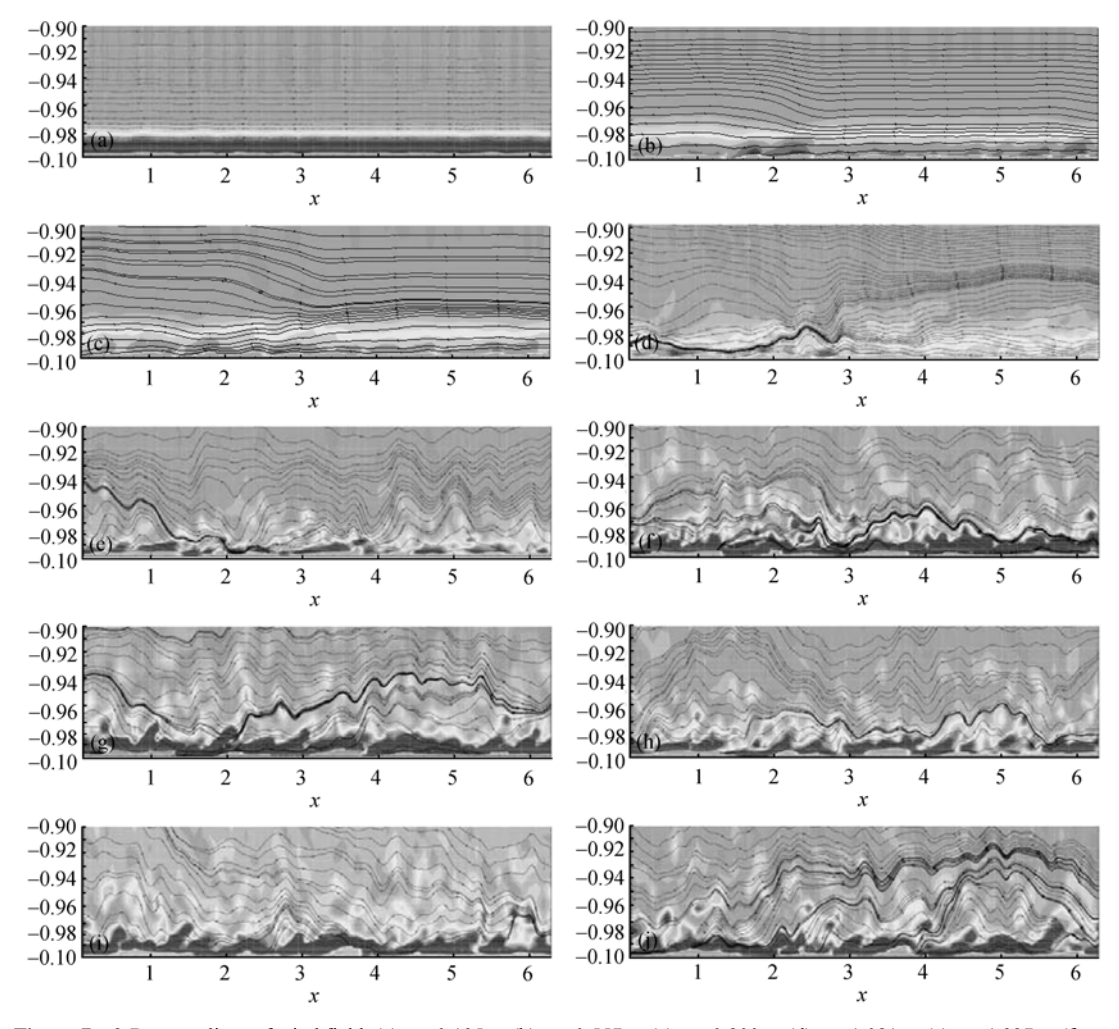


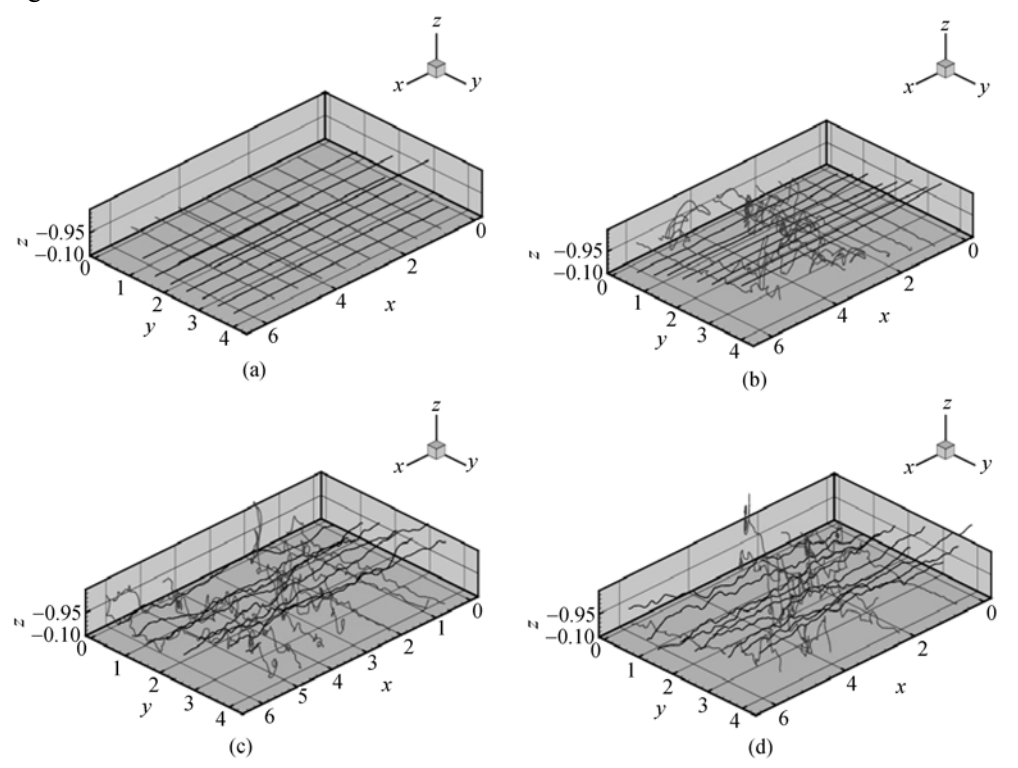
Figure 6 The vector diagram of a section of turbulent wind field.



**Figure 7** 2-D streamlines of wind field. (a) t = 0.195 s; (b) t = 0.557 s; (c) t = 0.800 s; (d) t = 1.081 s; (e) t = 1.327 s; (f) t = 1.440 s (g) t = 1.555 s; (h) t = 1.676 s; (i) t = 1.806 s; (j) t = 1.948 s.

Figure 8 shows 3-D streamlines and 3-D vortex lines, i.e., the lines along x direction are streamlines, and the ones perpendicular to streamlines are vortex lines. In Figures 8(a)—(d), one can see the variation process of sand ripples from low to high, and at the same time the obvious changes of streamlines and vortex lines are observed. In Figure 8(a) the streamlines are completely parallel to the flow direction without any inclination or fluctuation, and the vortex lines are exactly perpendicular to the streamlines, which shows that the flow is not affected by the small wavy ups

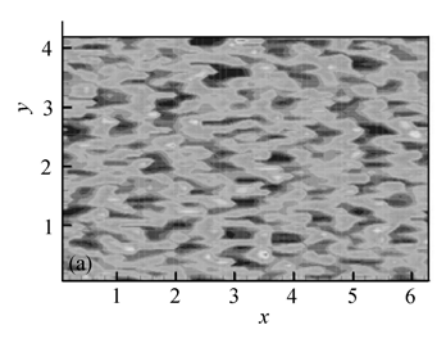
and downs on the ground. In Figure 8(b), the streamlines have slight wavy motion, and the variation of vortex lines is far more distinct from straight to winding, but their positions are still close to the ground, which means that the vortices generated by the interactions of turbulent field and sand ripples only influence the near ground wind field. Due to full development of sand ripples, the vertical fluctuations of streamlines in Figures 8(c) and (d) are more obvious, and vortex lines extend to higher positions, which signifies that due to the appearance and development of sand ripples, there is stronger energy exchange of turbulence in the vertical direction, and this might be one of the mechanisms of sand storms starting up. The interactions between sand ripples and near ground turbulent vortex structures are very complicate, and need further study. From Figure 9, we can find that there are strong correspondences between near ground vorticity and sand ripples, which once again shows the understanding that sand ripples are the imprints of turbulent wind field left on the desert ground.



**Figure 8** 3-D streamlines and 3-D vortex lines. (a) t = 0.557 s; (b) t = 0.915 s; (c) t = 1.806 s; (d) t = 2.096 s.

#### 5 Conclusions

With the method of large-eddy simulation, the equation of spherule motion and the method of immersed boundary, numerical simulations of three-dimensional turbulent aeolian motion are carried out, together with the studies of the formation of sand ripples under three-dimensional turbulent wind and the mutual actions of saltation and creeping motion. The resulting sand ripples have the form identical to the sand ripples in nature, which is flat on the upwind side and steep on the leeward. We also realized the self-restoration process of three-dimensional sand ripples, which shows the correctness of the methods of numerical simulations and the models of saltation and creeping. Finally, We analyzed the influence of sand ripples on the three-dimensional turbulent



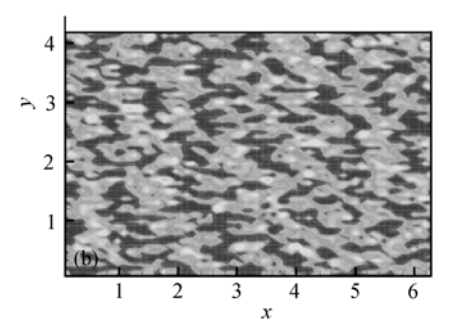


Figure 9 The 2-D projection of sand ripples and the vorticity near the ground at t = 1.676 s. (a) The 2-D projection of sand ripples; (b) the vorticity near the ground.

wind field, and found that due to the appearance and development of sand ripples, in the normal direction of ground there exist stronger turbulent energy exchanges, and moreover, there is close correspondence between the forms of sand ripples and the vorticity close to the ground surface, which might be useful for understanding the mechanism of sand storms starting.

We appreciate the valuable suggestions of the referees.

- 1 Ling Y Q, Qu J J, Li C Z. Study on sand ripple movement with close shoot method. J Desert Res (in Chinese), 2003, 23(2): 118-120
- 2 Sun X K, Zhang K, Zhang D Z, et al. Review on trajectory theory of sand-ripple formation. J Desert Res (in Chinese), 2003, 23(4): 471-475
- 3 Yang B, Zou X Y, Dong G R. Advances and problems of study on saltation particles in wind-sand current. J Desert Res (in Chinese), 1999, 19(2): 173-177
- 4 Anderson R S. A theoretical model for aeolian impact ripples. Sedimentology, 1987, 34: 943 956[DOI]
- 5 Anderson R S. Eolian ripples as examples of self-organization in geo-morphological systems. Earth Sci Rev, 1990, 29: 77-96
- 6 Haff P K, Anderson R S. Grain scale simulation of loose sedimentary bed, the example of grain-bed impacts in aeolian saltation. Sedimentology, 1993, 40: 175–198[DOI]
- 7 Zheng X J, Xie L, Zou X Y. Theoretical prediction of liftoff angular velocity distributions of sand particles in wind-blown sand flux. J Geophys Res, 2006, 111: D11109[D01]
- 8 Zheng X J, He L H, Wu J J. Vertical profiles of mass flux for windblown sand movement at steady state. J Geophys Res, 2004, 109: B01106[DOI]
- 9 Zheng X J, Huang N, Zhou Y H. Laboratory measurement of electrification of wind-blown sands and simulation of its effect on and saltation movement. J Geophys Res, 2003, 108: D104322
- 10 Nishimori H, Ouchi H. Formation of ripple patterns and dunes by wind-blown sand. Phys Rev Lett, 1993, 71(1): 197–200 [DOI]
- 11 Walter L, Werner B T. Computer simulations of self-organized wind ripple patterns. Phys D, 1994, 77: 238 260[DOI]
- 12 Nino Y, Atala Y. Discrete computer simulations of ripple emergence and evolution. In: The 27th Congress of the International Association for Hydraulic Research. New York: ASCE, 1997. 1179—1184
- 13 Ran Q H. Computer simulations of aeolian sand ripples (in Chinese). Thesis for Master Degree. Beijing: Tsinghua University, 1999
- 14 Wang G Q, Ran Q H, Liu L B. Computer simulations of aeolian sand ripples. J Sediment Res (in Chinese), 1998, 3: 1-6
- 15 Sun Q C, Wang G Q. Numerical simulation of aeolian sediment transport. Chin Sci Bull, 2001, 46(9): 786—788
- 16 Liu N Y. Large-eddy simulation of turbulent share flows in plane channels with buoyancy effect (in Chinese). Dissertation for the Doctoral Degree. Hefei: University of Science and Technology of China, 1998
- 17 Peskin C S. Flow patterns around heart valves: A digital computer method for solving the equations of motion. PhD Thesis, Physiol. New York: Albert Einstein Coll. Med., Univ. Microfilms, 1972, 378: 72-30
- 18 Mittal R, Iaccarino G. Immersed boundary methods. Ann Rev Fluid Mech, 2005, 37: 239 261[DOI]
- 19 Goldstein D, Handler R, Sirovich L. Modeling a no-slip flow boundary with an external force field. J Comput Phys, 1993, 105: 354—366[DOI]
- 20 White F M. Viscous Fluid Flow. New York: McGraw-hill Book Company, 1979
- 21 Shao Y. Physics and Modelling of Wind Erosion. Dordrecht: Kluwer Academic, 2000
- 22 Anderson R S, Hallet B. Sediment transport by wind: toward a general model. Bull Geol Soc Am, 1986, 97: 523-535[DOI]
- 23 Schmidt D S, Schmidt R A, Dent J D. Electrostatic force on saltating sand. J Geophys Res, 1998, 103: 8997—9001[DOI]
- 24 He L H. Coupled interaction of wind velocity-sand movement-electric field and its influence on windblown sand saltation (in Chinese). Dissertation for the Doctoral Degree. Lanzhou: Lanzhou University, 2005